

Numerical evaluation of conservation properties for a Primal Hybrid method for the Biot system

Maicon R. Correa¹, Giovanni Taraschi²

¹*Departamento de Matemática Aplicada, IMECC, Unicamp
Rua Sérgio Buarque de Holanda, 651, 13083-859, Campinas/SP, Brasil
maicon@ime.unicamp.br*

²*Laboratório de Mecânica Computacional, FECFAU, Unicamp
Rua Saturnino de Brito, 224, 13083-889, Campinas/SP, Brasil
taraschi@unicamp.com*

Abstract. In this work, we evaluate local conservation properties of numerical approximations for the Biot system in two dimensions. The numerical approximations are obtained using a Primal Hybrid Finite Element method in terms of displacement and pressure, on quadrilateral partitions of the domain. The total stress and Darcy velocity are locally post-processed by solving simple problems at the element level. Our results indicate that this methodology leads to locally conservative solutions for the dual variables (stress and velocity).

Keywords: Poroelasticity, Biot system, Primal Hybrid method, Locally conservative approximations

1 Introduction

Let $\Omega \subset \mathbb{R}^2$ be a polygonal and bounded domain representing a linearly elastic porous medium saturated by an incompressible Newtonian fluid, and $t_f > 0$ be a given final time instant. The Biot model for consolidation [1] describes the interaction between the deformation of the porous matrix and the fluid flow via the following system of differential equations,

$$\operatorname{div}(\mathbf{C}\boldsymbol{\varepsilon}(\mathbf{u})) - \alpha \nabla p = \mathbf{f}, \quad \text{in } \Omega \times (0, t_f], \quad (1a)$$

$$\frac{\partial}{\partial t}(\alpha \operatorname{div} \mathbf{u}) - \operatorname{div}(\mathcal{K} \nabla p) = g, \quad \text{in } \Omega \times (0, t_f], \quad (1b)$$

where the variables of interest are the displacement vector $\mathbf{u} : \Omega \rightarrow \mathbb{R}^2$ and the pore pressure $p : \Omega \rightarrow \mathbb{R}$. Here, \mathbf{C} is the fourth-order elasticity tensor, \mathcal{K} is the second-order hydraulic conductivity tensor, $\boldsymbol{\varepsilon}(\mathbf{u})$ is the infinitesimal strain tensor (given by the symmetric part of $\nabla \mathbf{u}$), α is the Biot-Willis constant, and \mathbf{f} and g are the load and source/sink functions, respectively. Equations (1a) and (1b) represent the equilibrium and the overall mass balance of the system, respectively. Alongside these equations, one must consider boundary and initial conditions to obtain a well-posed problem [2, 3]. For simplicity, we shall set homogeneous Dirichlet boundary conditions for both \mathbf{u} and p and assume that the initial values $\mathbf{u}(\mathbf{x}, 0)$ and $p(\mathbf{x}, 0)$ are known.

2 Primal Hybrid method

Given \mathcal{T}_h a quadrilateral mesh for Ω with no hanging nodes, the traditional way to approximate (1) uses the classical H^1 -conforming Finite Element method to discretize in space [1, 2], where both \mathbf{u} and p are approximated by continuous functions. Other possible approximations, based on mixed finite element methods and Discontinuous Galerkin schemes can be found, for example, in [3–5]. In this work, however, we propose the use of a Primal Hybrid strategy, which was first analyzed for the Poisson problem in [6] and recently applied to the elasticity and to transient problems [7–9].

When applied to the Biot system, the proposed Primal Hybrid method relies on the broken scalar and vector-valued approximation spaces

$$\mathcal{X}_h^{D,s} = \{v \in L^2(\Omega) : v|_K \in \mathcal{Q}_K^s, \forall K \in \mathcal{T}_h\} \quad (2)$$

and

$$\mathcal{X}_h^{E,r} = \mathcal{X}_h^{D,r} \times \mathcal{X}_h^{D,r}. \quad (3)$$

Here, \mathcal{Q}_K^s denotes the space obtained by mapping the polynomials of degree at most s in each coordinate from a reference square element \hat{K} to the geometrical elements K [10, 11]. The continuity of both the displacement and pressure fields is weakly imposed using the spaces

$$\mathcal{M}_h^{D,s} = \left\{ l \in \prod E_s(\partial K) : l|_{\partial K_1} + l|_{\partial K_2} = 0 \text{ for every pair of neighboring elements } K_1 \text{ and } K_2 \right\} \quad (4)$$

and its vector-valued counterpart

$$\mathcal{M}_h^{E,r} = \mathcal{M}_h^{D,r} \times \mathcal{M}_h^{D,r}, \quad (5)$$

where $E_s(\partial K)$ denotes the space defined over the boundary ∂K composed by functions that are polynomials of degree at most s when restricted to each edge of K .

For $r \geq 2$ and $s \geq 1$ two integers, the considered Primal Hybrid method reads: for each $n = 1, \dots, N$, find $(\mathbf{u}_h^n, \mathbf{m}_h^{E,n}, p_h^n, m_h^{D,n}) \in \mathcal{X}_h^{E,r} \times \mathcal{M}_h^{E,r-1} \times \mathcal{X}_h^{D,s} \times \mathcal{M}_h^{D,s-1}$ satisfying

$$(\mathbf{C}\varepsilon(\mathbf{u}_h^n), \varepsilon(\mathbf{v}))_{\mathcal{T}_h} - (\mathbf{m}_h^{u,n}, \mathbf{v})_{\partial\mathcal{T}_h} + (\alpha p_h^n, \text{div } \mathbf{v})_{\mathcal{T}_h} = -(\mathbf{f}^n, \mathbf{v})_{\Omega}, \quad \forall \mathbf{v} \in \mathcal{X}_h^{E,r}, \quad (6a)$$

$$\langle \mathbf{l}, \mathbf{u}_h^n \rangle_{\partial\mathcal{T}_h} = 0, \quad \forall \mathbf{l} \in \mathcal{M}_h^{E,r-1}, \quad (6b)$$

$$(\mathcal{K} \nabla p_h^n, \nabla q)_{\mathcal{T}_h} + (m_h^{p,n}, q)_{\partial\mathcal{T}_h} + \frac{\alpha}{\Delta t} (\text{div } \mathbf{u}_h^n, q)_{\mathcal{T}_h} = (g^n, q)_{\Omega} + \frac{\alpha}{\Delta t} (\text{div } \mathbf{u}_h^{n-1}, q)_{\mathcal{T}_h}, \quad \forall q \in \mathcal{X}_h^{D,s}, \quad (6c)$$

$$\langle l, p_h^n \rangle_{\partial\mathcal{T}_h} = 0, \quad \forall l \in \mathcal{M}_h^{D,s-1}, \quad (6d)$$

where we employ the broken products

$$(p, q)_{\mathcal{T}_h} = \sum_{K \in \mathcal{T}_h} \int_K p q \, dx \quad (7)$$

and

$$\langle m, l \rangle_{\partial\mathcal{T}_h} = \sum_{K \in \mathcal{T}_h} \int_{\partial K} m l \, ds, \quad (8)$$

which naturally extend for vector-valued functions as well. In addition to the space discretization, system (6) uses the backward Euler method for time discretization, with $\Delta t = t_f/N$ being the time step and the index n added to indicate that the relevant functions are being computed on $t_n = n\Delta t$. We refer to [12] for further details.

2.1 Velocity and Stress recovery

One of the main features of (6) is that the hybrid variables \mathbf{m}_h^E and m_h^D carry a physical meaning, being associated with the normal application of the total stress and the normal flux, respectively. This enables a local post-processing to recover $H(\text{div})$ -conforming approximations for the total stress tensor and the Darcy velocity. To illustrate the ideas, we shall use the classical Raviart-Thomas vector spaces \mathcal{RT}_s , defined on the reference square as the space

$$P_{s+1,s}(\hat{K}) \times P_{s,s+1}(\hat{K}),$$

where $P_{s,r}(\hat{K})$ is the space of polynomials with degree at most s in the first coordinate and at most r in the second one. The global spaces are constructed by mapping the reference space using the Piola transform and imposing the continuity of the normal component [11]. We shall use the same notation \mathcal{RT}_r to refer to the tensor version of these spaces, composed by 2×2 tensors which each row is a Raviart-Thomas vector. For a detailed construction of such spaces, we refer to [13].

Following the ideas of [11, 12, 14], approximations $\boldsymbol{\sigma}_h^{T,n} \in \mathcal{RT}_{r-1}$ and $\boldsymbol{\zeta}_h^n \in \mathcal{RT}_{s-1}$ for the total stress and the Darcy velocity can then be obtained by solving the local problems

$$\int_{\partial K} (\boldsymbol{\zeta}_h^n|_K \cdot \mathbf{n}^{\partial K}) l \, ds = \int_{\partial K} m_h^{D,n} l \, ds, \quad \forall l \in E_{s-1}(\partial K), \quad (9a)$$

$$\text{(if } s \geq 2) \quad \int_K \boldsymbol{\zeta}_h^n|_K \cdot \boldsymbol{\psi} \, dx = - \int_K (\mathcal{K} \nabla p_h^n) \cdot \boldsymbol{\psi} \, dx, \quad \forall \boldsymbol{\psi} \in \boldsymbol{\Psi}_{s-1}. \quad (9b)$$

and

$$\int_{\partial K} (\boldsymbol{\sigma}_h^{T,n}|_K \mathbf{n}^{\partial K}) \cdot \mathbf{l} \, ds = \int_{\partial K} \mathbf{m}_h^{E,n} \cdot \mathbf{l} \, ds, \quad \forall \mathbf{l} \in E_{r-1}(\partial K) \times E_{r-1}(\partial K), \quad (10a)$$

$$\text{(if } r \geq 2) \quad \int_K \boldsymbol{\sigma}_h^{T,n}|_K : \boldsymbol{\psi} \, dx = \int_K (\mathbf{C}\varepsilon(\mathbf{u}_h^n) + p_h^n \mathbf{I}) : \boldsymbol{\psi} \, dx, \quad \forall \boldsymbol{\psi} \in \boldsymbol{\Psi}_{r-1} \times \boldsymbol{\Psi}_{r-1}, \quad (10b)$$

respectively, where $\mathbf{n}^{\partial K}$ is the outward unitary normal over ∂K and the auxiliary space Ψ_{s-1} is defined as

$$\Psi_{s-1} = \{DF_K^t \hat{\boldsymbol{\tau}} \circ F_K^{-1} : \hat{\boldsymbol{\tau}} \in P_{s-2,s-1}(\hat{K}) \times P_{s-1,s-2}(\hat{K})\}. \quad (11)$$

In the definition (11), F_K is the mapping between \hat{K} and K and DF_K its Jacobian matrix.

3 Numerical experiment

The main goal of this section is to illustrate, through a simple numerical example, balance properties of the approximations obtained by (9) and (10) from the Primal Hybrid solution. For that, we shall first consider a coarse mesh of 4×4 square elements for the domain $\Omega = (0, 1) \times (0, 1)$, and set the polynomial orders $r = 2$ and $s = 1$. We also set \mathcal{K} as the identity tensor, \mathcal{C} as the isotropic elasticity tensor with Lamé coefficients $\mu = 1$ and $\lambda = 0.3$, and $\alpha = 1$. Functions \mathbf{f} and g are chosen such that the exact solutions for the displacement and pressure are given by

$$\mathbf{u}(x, y) = \begin{bmatrix} t \sin(\pi x) \sin(\pi y) \\ t \sin(\pi x) \sin(\pi y) \end{bmatrix}$$

and

$$p(x, y) = \frac{t}{2} \exp(x + y).$$

Since the exact solutions are linear in t we perform only one time iteration to reach the final instant $t_f = 1$.

Considering $\mathbf{1}$ the vector with unitary entries and $\text{asym}(\boldsymbol{\tau}) = \boldsymbol{\tau}_{1,2} - \boldsymbol{\tau}_{2,1}$ a measurement for the skew-symmetric part of $\boldsymbol{\tau} \in \mathbb{R}^{2 \times 2}$, in Figure 1 we plot the quantities

$$\left| \int_K \text{div } \boldsymbol{\zeta}_h^n - g^n + \frac{\alpha}{\Delta t} \text{div}(\mathbf{u}_h^n - \mathbf{u}_h^{n-1}) \, dx \right|, \quad (12)$$

$$\left| \int_K (\text{div } \boldsymbol{\sigma}_h^{T,n} - \mathbf{f}^n) \cdot \mathbf{1} \, dx \right|, \quad (13)$$

and

$$\left| \int_K \text{asym}(\boldsymbol{\sigma}_h^{T,n}) \, dx \right| \quad (14)$$

on each mesh element for $t = t_f$, which measure the violation of mass, linear momentum, and angular momentum conservation, respectively.

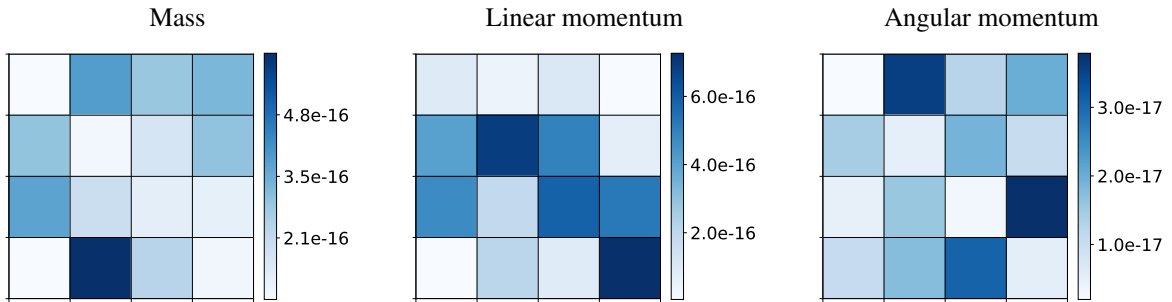


Figure 1. Violation measurements defined in (12), (13), and (14), plotted on each element.

Our results indicate that, even for a very coarse mesh, the approximated fields leads to local conservation of the quantities (12), (13), and (14). Concerning the measure (12), it is important to note that local conservation holds in the sense that the approximate solutions for $\boldsymbol{\zeta}_h^n$, \mathbf{u}_h^n and \mathbf{u}_h^{n-1} satisfy exactly the discrete form of the original mass balance (1b). It is equivalent to saying that these fields satisfy the balance

$$\int_{\partial K} \left(\boldsymbol{\zeta}_h^n + \frac{\alpha}{\Delta t} (\mathbf{u}_h^n - \mathbf{u}_h^{n-1}) \right) \cdot \mathbf{n} \, ds = \int_K g^n \, dx$$

at element level. For the particular case of a rigid porous medium with no external source of mass ($g = 0$), this balance reduces to the usual local mass conservation property of Darcy flow

$$\int_{\partial K} \boldsymbol{\zeta}_h^n \cdot \mathbf{n} \, ds = 0.$$

In addition to good conservation properties, the proposed method also has solid convergence behavior in space. To illustrate that, we consider $N_\Omega \times N_\Omega$ square meshes and measure how the approximation errors decay as the mesh is refined. We use the L^2 norm to measure the convergence rates of \mathbf{u}_h^n and p_h^n , and the $H(\text{div})$ norm for the convergence of $\boldsymbol{\sigma}_h^n$ and $\boldsymbol{\zeta}_h^n$. The results are shown in Table 1. Notice that the convergence rates for both the total stress and the Darcy velocity are the best ones possible, considering the approximation spaces chosen.

Table 1. Spatial convergence of the approximations u_h^n , p_h^n , $\boldsymbol{\sigma}_h^n$ and $\boldsymbol{\zeta}_h^n$.

N_Ω	$\ \mathbf{u}^n - \mathbf{u}_h^n\ _0$		$\ p^n - p_h^n\ _0$		$\ \boldsymbol{\sigma}^{T,n} - \boldsymbol{\sigma}_h^{T,n}\ _{H(\text{div})}$		$\ \boldsymbol{\zeta}^n - \boldsymbol{\zeta}_h^n\ _{H(\text{div})}$	
	err.	rate	err.	rate	err.	rate	err.	rate
2	2.40e-02	-	5.17e-02	-	3.13e+00	-	7.23e-01	-
4	3.33e-03	2.9	1.31e-02	2.0	8.05e-01	2.0	3.64e-01	1.0
8	4.53e-04	2.9	3.30e-03	2.0	2.03e-01	2.0	1.82e-01	1.0
16	6.09e-05	2.9	8.26e-04	2.0	5.07e-02	2.0	9.11e-02	1.0
32	8.63e-06	2.8	2.06e-04	2.0	1.27e-02	2.0	4.56e-02	1.0
64	1.44e-06	2.6	5.16e-05	2.0	3.17e-03	2.0	2.28e-02	1.0

4 Conclusions

In this work we propose a Primal Hybrid method to solve the Biot system. We show that the total stress and the Darcy velocity can be recovered by a simple local post-processing strategy, resulting in globally $H(\text{div})$ -conforming approximations. Such approximations converge optimally in the $H(\text{div})$ norm for square meshes and are locally conservative. We conclude that the Primal Hybrid method is a viable option to solve the Biot's system, specially when good approximations for the dual variables (stress and velocity) are desired, at selected time steps.

Acknowledgements. The authors thankfully acknowledge financial support from National Council for Scientific and Technological Development - CNPq (under grants 304192/2019-8, 132625/2019-9, 140400/2021-4, and 307679/2023-3) and ExxonMobil through FUNCAMP (process 48530-25).

Authorship statement. The authors hereby confirm that they are the sole liable persons responsible for the authorship of this work, and that all material that has been herein included as part of the present paper is either the property (and authorship) of the authors, or has the permission of the owners to be included here.

References

- [1] M. A. Murad and A. F. Loula. Improved accuracy in finite element analysis of Biot's consolidation problem. *Computer Methods in Applied Mechanics and Engineering*, vol. 95, n. 3, pp. 359–382, 1992.
- [2] M. A. Murad, V. Thomée, and A. F. Loula. Asymptotic behavior of semidiscrete finite-element approximations of Biot's consolidation problem. *SIAM journal on numerical analysis*, vol. 33, n. 3, pp. 1065–1083, 1996.
- [3] M. Jayadharan, E. Khattatov, and I. Yotov. Domain decomposition and partitioning methods for mixed finite element discretizations of the biot system of poroelasticity. *Computational Geosciences*, vol. 25, n. 6, pp. 1919–1938, 2021.
- [4] P. J. Phillips and M. F. Wheeler. A coupling of mixed and continuous Galerkin finite element methods for poroelasticity I: the continuous in time case. *Computational Geosciences*, vol. 11, n. 2, pp. 131–144, 2007.
- [5] P. J. Phillips and M. F. Wheeler. A coupling of mixed and discontinuous Galerkin finite-element methods for poroelasticity. *Computational Geosciences*, vol. 12, n. 4, pp. 417–435, 2008.
- [6] P.-A. Raviart and J.-M. Thomas. Primal hybrid finite element methods for 2nd order elliptic equations. *Mathematics of computation*, vol. 31, n. 138, pp. 391–413, 1977.
- [7] C. Harder, A. L. Madureira, and F. Valentin. A hybrid-mixed method for elasticity. *ESAIM: Mathematical Modelling and Numerical Analysis*, vol. 50, n. 2, pp. 311–336, 2016.
- [8] S. K. Acharya and K. Porwal. Primal hybrid finite element method for the linear elasticity problem. *Applied mathematics and Computation*, vol. 435, pp. 127462, 2022.

- [9] S. K. Acharya and A. Patel. Primal hybrid method for parabolic problems. *Applied Numerical Mathematics*, vol. 108, pp. 102–115, 2016.
- [10] G. Taraschi and M. R. Correa. On the convergence of the primal hybrid finite element method on quadrilateral meshes. *Applied Numerical Mathematics*, vol. 181, pp. 552–560, 2022.
- [11] M. R. Correa and G. Taraschi. Optimal H(div) flux approximations from the primal hybrid finite element method on quadrilateral meshes. *Computer Methods in Applied Mechanics and Engineering*, vol. 400, pp. 115539, 2022.
- [12] G. Taraschi. *Primal Hybrid Methods with Stress Recovery for Nearly Incompressible Elasticity and Poroe-lasticity*. PhD thesis, Universidade Estadual de Campinas. In Portuguese, 2025.
- [13] G. Taraschi, M. R. Correa, A. Pinto, and C. O. Faria. A global H(div)-conforming finite element post-processing for stress recovery in nearly incompressible elasticity. *Applied Mathematics and Computation*, vol. 470, pp. 128587, 2024.
- [14] S.-H. Chou, D. Y. Kwak, and K. Y. Kim. Flux recovery from primal hybrid finite element methods. *SIAM Journal on Numerical Analysis*, vol. 40, n. 2, pp. 403–415, 2002.